Neurobiology

Synaptic Changes in Alzheimer's Disease

Increased Amyloid-β and Gliosis in Surviving Terminals Is Accompanied by Decreased PSD-95 Fluorescence

Karen Hoppens Gylys,*[†] Jeffrey A. Fein,*
Fusheng Yang,[‡] Dorothy J. Wiley,*
Carol A. Miller,[§] and Gregory M. Cole[‡]

From the University of California at Los Angeles School of Nursing and Brain Research Institute,[†] UCLA School of Medicine, Los Angeles; the Departments of Pathology, Neurology, and Program in Neuroscience,[§] the Keck USC School of Medicine, Los Angeles, California; and the Department of Medicine and Neurology, UCLA School of Medicine and Sepulveda Veteran's Administration Medical Center,[‡] Sepulveda, California*

In an effort to examine changes that precede synapse loss, we have measured amyloid-β and a series of damage markers in the synaptic compartment of Alzheimer's disease (AD) cases. Because localization of events to the terminal region in neurons is problematic with conventional methods, we prepared synaptosomes from samples of cryopreserved human association cortex, and immunolabeled terminals with a procedure for intracellular antigens. Fluorescence was quantified using flow cytometry. The viability dye calcein AM was unchanged in AD terminals compared to controls, and the fraction of large synaptosome particles did not change, although a striking loss of large terminals was observed in some AD cases. The percent positive fraction for a series of pre- and postsynaptic markers was not affected by AD in this cohort. However, the amyloid-β-positive fraction increased from 16 to 27% (*P* < 0.02) in terminals from AD cortex. The expression level on a per-terminal basis is indicated in this assay by fluorescence (relative fluorescence units). The fluorescence of presynaptic markers did not change in AD terminals, but PSD-95 fluorescence was decreased by 19% (*P* < 0.03). Amyloid-β fluorescence was increased by 132% (*P* < 0.01), and glial fibrillary acidic protein labeling by 31% (*P* < 0.01). These results suggest that synapse-associated amyloid-β is prominent in regions relatively unaffected by AD lesions, and that amyloid accumulation in surviving terminals is accompanied by

gliosis and alteration in the postsynaptic structure. (*Am J Pathol 2004, 165:1809–1817*)

Despite abundant evidence supporting the amyloid cascade hypothesis, the early molecular events that occur in Alzheimer's disease (AD) are not clear.[1] Loss of synaptic terminals in AD brains demonstrates a higher correlation with decreased cognitive function than cell death or plaque development, which has led to the hypothesis that disappearance of synapses is a key event in early cognitive decline.[2] The best correlate of synapse loss in AD is soluble rather than fibrillar forms of amyloid-β protein (Aβ).[3] Transgenic mouse models that overexpress mutant or wild-type amyloid precursor protein (APP) have shown that synapse loss correlates with increased levels of soluble Aβ rather than either APP level or amyloid deposits. Further, synapse loss occurred even in the absence of amyloid deposition.[4] The cellular location of initial amyloid-related damage is controversial, but a growing body of evidence suggests that intracellular accumulation of Aβ precedes plaque formation.[5,6] Recent studies showing that perforant path and entorhinal cortical lesions reduce amyloid deposition in terminal fields of transgenic mice provide additional support for the hypothesis that deposited amyloid may originate in the synaptic compartment.[7,8] However, the mechanism of synapse loss in AD remain uncertain.

A large body of evidence supports the hypothesis that the memory failure of AD, particularly early impairment, is a result of synaptic dysfunction and loss, which is usually

Table 1. Case Information for Synaptosome Samples

No.	Sex	Age (years)	PMI (hours)	MMSE	Frontal Atrophy	Frontal Plaques	Amyloid fluor. in terminals (RFU)
Controls							
1	F	84	6	27	None	None	18.05
2	F	91	4.4	29	Mod	Mod	25.95
3	M	69	6.25	28	Mild	None	19.93
4	M	90	10.75	27	None	None	18.21
5	F	91	9	–	Mild	Sparse	13.45
6	F	92	7	25	None	None	16.46
7 (Parkinson's)	F	83	5.17	12	Mod	Sparse	50.9
8 (Parkinson's)	M	79	3.3	–	Mild	Sparse	25.43
Alzheimer's cases							
1	F	77	4.25	7	Mod	Mod	40.25
2	F	86	6	6	Mild	Mod	–
3	M	83	4	–	Mild	Mod	46.1
4	F	81	3.7	–	Mod	Mod	49.65
5	F	78	4.5	–	Mod	Mod	24.58
6	F	90	3.28	15	Mild	Freq	30.29
7	F	80	3.4	0	Severe	Freq	67.88
8	M	85	4.3	5	Mod	Mod	95.27
9	M	66	5	1	Mild	Mod	69.96
10	F	85	3.7	–	Severe	Mod	82.08

Plaque level refers to thioflavin-positive mature neuritic plaques with core; sparse (<5/field), mod (6 to 20/field), freq (21 to 30/field, or above). RFU, relative fluorescence units for 10G4 antibody fluorescence measured by flow cytometry.

measured by synaptophysin immunoreactivity.[9] On the other hand, presynaptic markers have also been shown to increase in early AD,[10] and synapse loss is often not detected in transgenic models.[11,12] Preferential loss of postsynaptic compared to presynaptic proteins in AD has been suggested based on decreases in drebrin, a postsynaptic actin-binding protein.[13–15] A role for caspase activation and apoptosis in AD cell death and neuritic damage is suggested by the detection of caspase-cleaved actin around plaques in AD-affected cortex and in APP transgenic mouse brain.[16] Localized caspase activation within terminals is supported by Aβ-induced caspase activation in neurites[17] and synaptosomes.[18]

We hypothesized that synapse loss is associated with localized neurotoxicity of terminal β-amyloid in the terminals. Because definitive localization of neuronal events to terminal regions is difficult with conventional methods, we prepared synaptosomes from cryopreserved human tissue. To examine surviving terminals for changes that occur before synapse loss, we measured viability markers and levels of synaptic, proapoptotic, and Aβ proteins using flow cytometry. Increased glial fibrillary acidic protein (GFAP) and Aβ immunoreactivity were observed in AD terminals. These changes were accompanied by selective synaptic marker alterations in surviving terminals, namely a decrease in expression of postsynaptic PSD-95.

Materials and Methods

The monoclonal anti-Aβ antibody 10G4 has been described previously,[19] and the 7A6 antibody[20] was provided by S. Schlossman (Dana Farber Cancer Institute, Boston, MA). Polystyrene microsphere size standards were purchased from Polysciences, Inc. (Warrington, PA). The viability dye calcein AM and Zenon mouse IgG labeling kits for dual labeling were purchased from Molecular Probes (San Diego, CA). The following monoclonal antibodies were purchased: anti-SNAP-25 (Sternberger Monoclonals Inc., Lutherville, MD), anti-PSD 95 (Upstate Biotechnology, Lake Placid, NY), anti-GFAP, anti-synaptophysin, and anti-syntaxin (Sigma, St. Louis, MO), anti-synaptobrevin (Chemicon, Temecula, CA), anti-BACE (R&D Systems, Inc., Minneapolis, MN), and anti-APP (3E9; Medical and Biological Laboratories Co., Ltd., Nagoya, Japan).

Human Brain Specimens

Samples of human association neocortex (Brodmann area 7 and area 9) were obtained at autopsy from the University of Southern California Alzheimer's Disease Research Center. Samples were obtained from 10 cases diagnosed clinically and histopathologically with AD (mean age, 84.9 years; mean postmortem delay, 6.48 hours), and from eight aged controls (mean age, 81.1 years; mean postmortem delay, 4.21 hours). Two control cases had a clinical and neuropathological diagnosis of Parkinson's disease and were included in all analyses as neurological controls. The mean mini-mental state examination (MMSE) for the control group was 24.7 (±2.6), and for the AD group was 5.1 (±2.2). Some AD patients were untestable. Ten independent experiments were performed and, when possible, experiments compared one AD case with one control case. Case details are presented in Table 1.

P-2 Preparation

Samples (1 g), were minced and slowly frozen on the day of autopsy in 10% dimethyl sulfoxide and 0.32 mol/L sucrose and stored at −70°C until homogenization on the day of the experiment. This procedure has been previously optimized for the preservation of human brain sam-

ples.[21] The P-2 (crude synaptosome) fraction was prepared as described previously;[22] briefly, samples were rapidly thawed and homogenized in ice-cold 0.32 mol/L sucrose in 10 mmol/L Tris buffer (pH 7.4) with protease inhibitors (2 mmol/L EGTA, 2 mmol/L EDTA, 0.2 mmol/L phenylmethyl sulfonyl fluoride, 4 μg/ml leupeptin, 4 μg/ml pepstatin, 5 μg/ml aprotinin, 20 μg/ml trypsin I). The tissue was homogenized in a Teflon/glass homogenizer (clearance, 0.1 to 0.15 mm) by eight gentle up and down strokes at 800 rpm. The homogenate was spun at 1000 $\times$ g for 10 minutes to remove nuclei and cell debris. The resulting supernatant was centrifuged at 10,000 $\times$ g for 20 minutes to obtain the crude synaptosomal pellet. The final pellet was washed with 2 ml of phosphate-buffered saline (PBS) and centrifuged (4 minutes, 2000 $\times$ g, 4°C) before immunolabeling.

Dye Labeling

Calcein AM (final concentration, 0.02 nmol/L) was diluted in Krebs-Ringer phosphate buffer (KRP; 118 mmol/L NaCl, 5 mmol/L KCl, 4 mmol/L $MgSO_4$, 1 mmol/L $CaCl_2$, 1 mmol/L KH_2PO_4, 16 mmol/L sodium phosphate buffer, pH 7.4, and 10 mmol/L glucose) and added to 5- to 10-μl aliquots of P-2 (total volume, 0.1 ml), incubated for 10 minutes at 4°C, then diluted in 0.5 ml of PBS for immediate flow cytometry analysis.

Immunolabeling of P-2 Fraction

P-2 aliquots were immunolabeled for flow cytometry analysis according to a method for staining of intracellular antigens.[23] Pellets were fixed in 0.25% buffered paraformaldehyde (1 hour, 4°C) and permeabilized in 0.2% Tween 20/PBS (15 minutes, 37°C). The monoclonal antibodies were diluted 1:1000 in 2% fetal bovine serum/ PBS. After a 30-minute incubation with primary antibody at 4°C, pellets were washed two times with 1 ml of 0.2% Tween 20/PBS, then incubated (20 minutes, 4°C) with secondary antibody (fluorescein isothiocyanate-conjugated anti-mouse IgG, Molecular Probes, San Diego, CA) followed by two additional washes before resuspension in KRP buffer for flow cytometry analysis. For the dual-labeling studies shown in Figure 1, antibodies were labeled directly with Alexa Fluor 488 or 647 reagents according to kit directions. This mixture was added to P-2 aliquots and incubated at room temperature for 30 minutes followed by two washes before flow cytometry analysis.

Biochemical Analyses

For Western analysis P-2 samples were electrophoresed on a 10% Tris-glycine acrylamide gel (20 μg/lane) under reducing conditions. Proteins were transferred to a polyvinylidene difluoride membrane (400 mA for 2 hours) before blocking in 10% nonfat dried milk and 0.1% gelatin in PBS for 1.5 hours at 37°C. After incubation with primary antibody for 3 hours at room temperature, blots were rinsed and incubated in horseradish peroxidase-
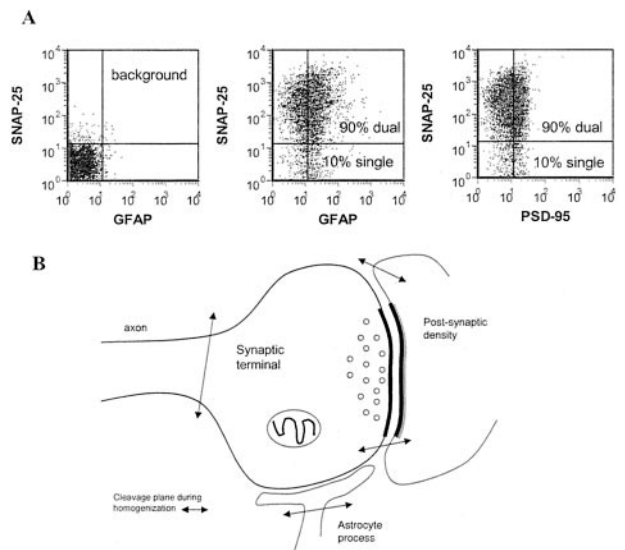

Figure 1. Presynaptic terminal in synaptosome preparation. Human cortical P-2 preparations immunolabeled for SNAP-25 were dual-labeled for GFAP (**A, middle**) and PSD-95 (**A, right**); background labeling is shown at the **left**. **B:** Illustration of synaptosome components; cleavage planes during homogenization are indicated by **arrows**.

conjugated goat anti-mouse (1:10,000) for 1 hour and then developed with enhanced chemiluminescence (Amersham Biosciences Corp., Piscataway, NJ). Films were scanned with the Bio-Rad GS-700 imaging densitometer (Bio-Rad Laboratories, Hercules, CA) and analysis of variance statistics analyzed with Statview version 5.0.1 (SAS Institute Inc., Cary, NC). The sandwich enzyme-linked immunosorbent assay for total Aβ has been described previously.[24] Briefly, the assay uses monoclonal 4G8 against Aβ17-24 (Senentek, Napa, CA) as the capture antibody (3 μg/ml), biotinylated 10G4 against Aβ1-15 as the detecting antibody, and a reporter system using streptavidin-alkaline phosphatase and AttoPhos (JBL Scientific Inc., San Luis Obispo, CA) as the substrate (excitation, 450 nm; emission, 580 nm). To measure insoluble Aβ, a 1:100 dilution of the guanidine-soluble extracts was made with Tris-buffered saline containing 5% bovine serum albumin and 1$\times$ protease inhibitor cocktail (Calbiochem, La Jolla, CA), then centrifuged (16,000 $\times$ g, 20 minutes, 4C).

Flow Cytometry

Analysis was performed using a FACSCalibur flow cytometer (Becton-Dickinson, San Jose, CA) equipped with a 488-nm argon laser and a 635-nm red diode laser. Sample flow rate was ~3000 events per second; 50,000 ungated events were collected for the analyses. A threshold was set on forward light scatter (channel 42) to exclude debris. Analysis was performed using FCS Express software (DeNovo Software, Ontario, Canada). Statistics were estimated from the data using the VassarStats web site for statistical computation (http://faculty.vassar.edu/ lowry/vassarstats.html).

Results

Synaptosomes from AD Cortex Are Intact and Esterase-Positive

A widely used method for the *in vitro* study of synaptic chemistry is the synaptosome preparation, which contains neuronal terminals that have resealed into a functional sphere during homogenization in isotonic sucrose (Figure 1). We have developed a method enabling quantitative analysis of synaptic markers in a P-2 homogenate using flow cytometry, and have recently compared synaptosomes from fresh rat and cryopreserved human tissue using our flow cytometry protocols.[26,27] Synaptosomes have historically been considered a preparation for the study of presynaptic neurochemistry. However, because the P-2 preparation has also been used to study postsynaptic proteins including the NMDA receptor and the dendritic spine protein RC3/neurogranin,[28,29] and because GFAP mRNA is enriched in hippocampal synaptosomes,[30] we have measured PSD-95, a postsynaptic scaffolding protein for the NMDA receptor, and GFAP, an astrocyte-specific intermediate filament protein, along with presynaptic neuronal proteins. Dual labeling of human cortical P-2 preparations from the present cohort reveals that both GFAP and PSD-95 co-localize with SNAP-25, confirming that synaptosomes possess adherent postsynaptic elements and astrocytic processes (Figure 1A). We did not observe differences in nonneuronal elements between control and AD cases (data not shown), and relatively few particles (~10%) contain only GFAP or PSD-95 (Figure 1A). Based on previous evidence[31] and the present dual-labeling results, typical cleavage planes that yield the particles analyzed in the synaptosome fraction are illustrated (Figure 1B).

Using a viability dye, calcein AM, that labels only intact, esterase-positive particles, we first examined the hypothesis that fewer intact synaptosome particles would be measured in AD cortex. Synaptosomes prepared from cryopreserved cortex were labeled with calcein AM and 50,000 particles from each sample were collected and analyzed by flow cytometry. Representative density plots are illustrated in Figure 2, A through C, for fluorescence versus forward scatter. Forward scatter is proportional to particle size, and the position of 0.75-, 1.4-, and 4.5-μm-size standards is shown in Figure 2C. The calcein-positive fraction of P-2 particles (Figure 2, A and B) was identified by an analysis gate based on background fluorescence in an unstained aliquot (Figure 2C). The viable fraction did not differ between AD and controls; 63% (±4.1, $n = 5$) of the P-2 fraction in controls was calcein-positive, compared to 65% (±3.6, $n = 7$) for AD cases. The ~65% integrity measured in cryopreserved human tissue compares to 90% in freshly prepared P-2 from rat brain,[25] an expected decline in viability, given the much longer postmortem interval (range, 3 to 10 hours) with human cases.[27]

Our previous work has shown that SNAP-25-positive particles vary from 0.5 to 5 μm in diameter, consistent with electron micrograph observations of synaptosome size. We next investigated the possibility that terminal
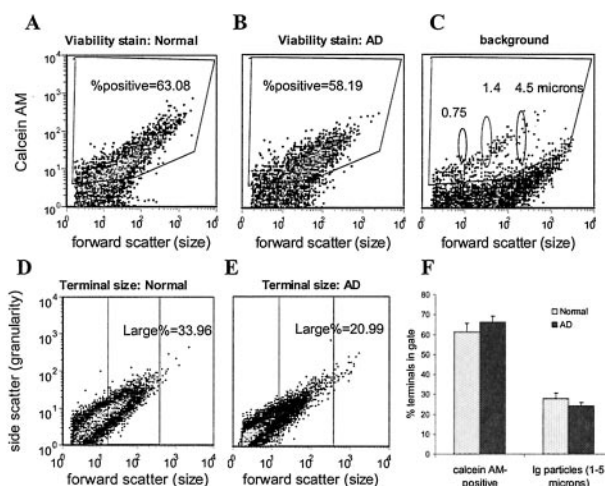

Figure 2. A–C: Synaptosomes from normal and AD cortex stain with the viability dye calcein AM. Flow cytometry analysis of calcein AM (30 nmol/L), which labels esterase-positive particles with an intact membrane. The data analysis gate is drawn to include specific labeling above background; percent positive indicates percentage of total particles specifically labeled for calcein AM. Forward scatter is proportional to particle size; data are from representative experiment with parallel measurements from normal and AD samples. **B–D:** Loss of large synaptosomes in AD. Synaptosomes 1- to 5-μm in size based on standards (shown in **C**) are enclosed within the center analysis gate; the percentage of total particles is indicated. Density plots illustrate loss observed in some cases (**B**, **C**); data from 10 independent experiments (50,000 events/sample) is summarized in graph **D**.

size varies in AD by drawing an analysis gate based on forward light scatter, which is proportional to size. The size-based gating analysis is illustrated in Figure 2, D and E, for representative control and AD cases. The largest particles are contained in the center analysis gate, which contains only particles ~1 to 5 μm in diameter (based on size standards illustrated in Figure 2C). In two AD cases, a striking loss in the fraction of large synaptosomal particles was observed (Figure 2, D and E), suggesting disappearance of large-diameter axonal terminals. This loss of large synaptosomes in AD (Figure 2, D and E) resembles the loss of large particles that we have observed with our flow cytometry analysis after treatment of synaptosomes *in vitro* with staurosporine.[32] However, the percentage of large synaptosomes was not decreased in the AD samples compared to controls: the mean large fraction was 27.9% (±2.8) in controls versus 24.2% (±1.8) in AD cases (Figure 2F).

Presynaptic Markers in AD Cortex Are Preserved Despite Accumulation of Aβ in Synaptic Terminals

Because flow cytometry measures fluorescence on a per-terminal basis, quantitative data are obtained in two dimensions: number of positives and brightness of fluorescence. Therefore, changes in the fraction of marker-expressing synaptosomes (percentage positive) can be detected as well as changes in expression level per terminal (indicated by relative fluorescence units). This is in contrast to conventional biochemical techniques and a key advantage of flow cytometry analysis.
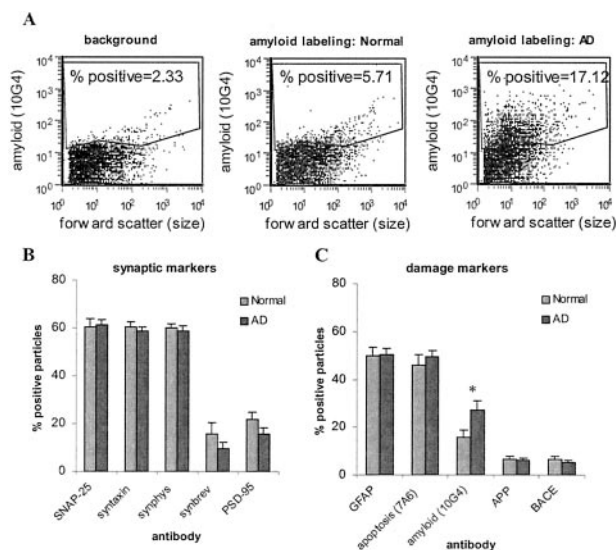
Figure 3. Size of percent-positive fraction for damage indicators in AD versus cognitively normal. The P-2 fraction was immunolabeled with antibodies directed against a series of markers for synapse damage and analyzed by flow cytometry. The positive fraction was identified using an analysis gate (**A**) to include particles labeled above background (**left**). Amyloid labeling is shown for a representative normal case (**middle**) and AD case (**right**). The size of the positive fraction is summarized for synaptic markers (**B**) and damage markers (**C**). Ten independent experiments were performed (50,000 events/sample); *, $P < 0.02$, Student's *t*-test.

To elucidate mechanisms of synaptic loss operating in AD brain, we immunolabeled synaptosome preparations and quantified the level of five synaptic markers and five damage indicators. Four presynaptic exocytotic proteins were measured in the present study: SNAP-25 and syntaxin, which are expressed along presynaptic axonal membranes (t-SNAREs), and synaptophysin and synaptobrevin, which are both integral membrane proteins on vesicles (v-SNAREs).[33] PSD-95, part of a scaffolding complex for the NMDA receptor,[34] was used to indicate postsynaptic changes. The damage indicators measured included GFAP as a measure of gliosis and the apoptosis antibody 7A6, which identifies an antigen that is expressed on the mitochondrial membrane of cells that are undergoing apoptosis.[20] Three proteins related to amyloid accumulation were measured: 1) the 10G4 antibody directed against residues 5 to 17 of the Aβ peptide,[19] the 3E9 antibody directed against residues 18 to 38 of the APP, and 3) the β-site APP-cleaving enzyme (BACE) that is required for the initial APP cleavage that releases Aβ peptide. The P-2 fraction was immunolabeled with monoclonal antibodies to each of these markers using a protocol for the staining of intracellular antigens in which gentle fixation is followed by permeabilization with a nonionic detergent.[23]

The positive fraction was identified by an analysis gate that excluded background labeling measured in the presence of an isotype-specific control antibody (Figure 3A, left), which also shows a representative AD versus normal comparison for Aβ labeling with the 10G4 antibody (Figure 3A, middle and right). Figure 3, B and C, shows the size of the positive fraction for synaptic markers and damage markers. The positive fraction for SNAP-25, syntaxin, and synaptophysin was almost identical,

with each labeling ~60% of the total P-2 particles. This result is consistent with the results in P-2 from fresh rat brain, and indicates presynaptic neuronal component to a majority of the particles in the homogenate.[25] In contrast, synaptobrevin labeled only 15% of the particles above background, suggesting a more restricted distribution. This result is consistent with immunocytochemical observation of limited synaptobrevin expression in the neuromuscular junction compared with syntaxin and SNAP-25.[35] Adherent postsynaptic elements are less frequent than presynaptic elements in the population, with PSD-95 labeling ~10% of the total.

An *in vivo* loss of synaptic terminals in AD cortex would be expected to result in fewer resealed presynaptic terminals in the homogenate compared to samples from normal cortex. Because the P-2 homogenate contains free vesicles and membrane fragments, and because flow cytometry acquisition was set up for random acquisition of 50,000 P-2 particles, synapse loss in the present assay would be detected as a decrease in the positive fraction for synaptic markers accompanied by an increase in the background fraction, which contains the nonsynaptosomal components in the P-2. AD did not significantly affect the percent positive fraction of any of the synaptic markers when the controls included the two Parkinson's cases (Figure 3B), although synaptobrevin labeling showed a nonsignificant 38% decrease in AD cases [from 15.8 ($\pm$4.7) to 9.7% ($\pm$2.7)]. PSD-95 labeling was nonsignificantly decreased by 28% [from 21.7 ($\pm$3.1) to 15.7 ($\pm$2.4)]. The decrease in both synaptobrevin becomes significant ($P < 0.05$, Student's *t*-test) if the demented Parkinson's case with MMSE = 12 is removed from the controls, and both synaptobrevin and PSD-95 are significantly reduced ($P < 0.05$, Student's *t*-test) when the two Parkinson's cases are removed from the control group, indicative of synaptic changes in the cortex of the aged Parkinson's patients in this cohort. Quantification of synapse number is technically difficult, and it is important to note that the exact relationship between our measure and the number of synapses per unit of cortical area is not clear. However, comparing four presynaptic markers in this assay, the positive fraction for synaptobrevin appears to be selectively altered by AD.

Figure 3C demonstrates that 50% ($\pm$3.0) of the particles in both AD and control groups possessed GFAP, a marker for astrocyte processes. Labeling of synaptosomal particles with GFAP is consistent with the intimate supportive role that astrocytes play for neurons, and is supported by electron microscope data showing close association of astrocyte processes with synaptic regions.[36,37] The proapoptotic antigen 7A6 fraction in synaptic terminals was not significantly affected by AD; however, the relatively high fraction of particles positive for the 7A6 antigen in the age-matched controls (46 $\pm$ 4.2%) was surprising and suggests the activation of synaptic proapoptotic pathways in the cognitively normal aged or possible postmortem effects. In freshly prepared rat synaptosomes, 7A6-positive terminals were fewer than 7% of the total (data not shown).

The fraction of terminals labeled for Aβ (Figure 3C) increased from 16% ($\pm$3.0) in aged controls to 27%
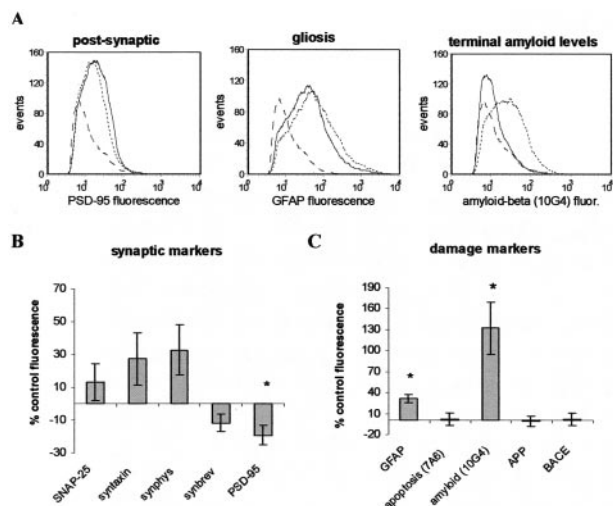
Figure 4. Per particle fluorescence changes in AD synaptic terminals. **A:** Histograms demonstrate fluorescence from a representative case-control comparison for labeling with: PSD-95 (**left**), GFAP (**middle**), and Aβ (10G4; **right**). **Dashed line** indicates isotype-specific background staining; **solid line** is labeling in normal age-matched control; **dotted line** is labeling in AD case. Synaptic marker (**B**) and damage marker (**C**) fluorescence in AD cases expressed as percentage of control; data from 10 independent experiments (50,000 events/sample) is summarized in graph; *, $P < 0.03$, Student's *t*-test.

Figure 5. Western analysis of P-2 fractions. Representative lanes are shown for seven cases in the cohort for PSD-95, GFAP, actin, and SNAP-25. Position of size standards is indicated in **middle**. Densitometric scanning did not reveal significant differences in expression level between normal cases ($n = 4$) and AD cases ($n = 7$).

(± 4.0; $P < 0.02$) in AD. It is interesting to note that in three of the eight normal controls, the number of Aβ-positive terminals was increased more than 24% (data not shown). Two of these three cases had a Parkinson's disease diagnosis and the demented Parkinson's patient with MMSE = 12 had grossly elevated terminal Aβ. Figure 3C shows that a relatively small percentage of synaptosomes labeled for APP ($7 \pm 1.4\%$) and BACE ($6 \pm 1.3\%$) in the control cases, and this fraction was not affected by AD. The precise localization of cellular Aβ has been difficult to determine; therefore, the presence of Aβ in surviving terminals suggests that synaptic accumulation of Aβ may be an indication of synaptic damage that precedes synapse loss in AD.

Presynaptic SNAP-25 Expression Is Preserved, but Synaptic Terminals from AD Cortex Exhibit Decreases in Postsynaptic Structure, Large Increases in Aβ, and Increased Gliosis

A change in the expression level of a damage marker in the population corresponds to a change in brightness or relative fluorescence. Figure 4A illustrates representative fluorescence histograms from a case-control comparison of synaptic damage indicators. In this comparison decreased fluorescence is observed in the AD case for the postsynaptic marker PSD-95 (Figure 4A, left) and increased fluorescence is measured for GFAP (Figure 4A, middle) and Aβ (Figure 4A, right). Background staining is indicated by the dashed line in each histogram; note that in this case the Aβ level is near background. We summarized fluorescence data from the entire cohort for synaptic markers in Figure 4B and for damage markers in Figure 4C. Presynaptic antigen expression was not sig-
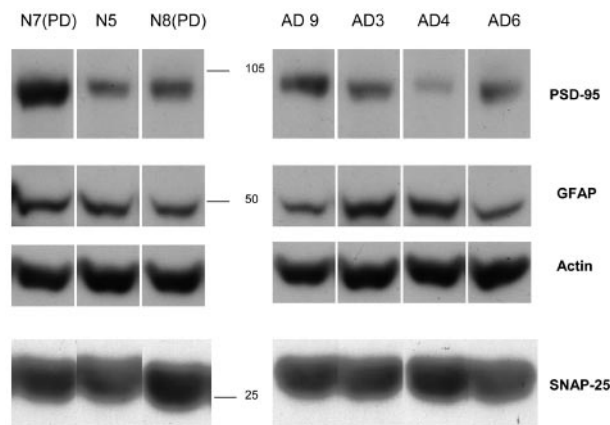
nificantly different in AD terminals, but PSD-95 expression associated with synaptosomes was decreased by 19% (± 5.9; $P < 0.03$) on this per-terminal basis. Because PSD-95 is an integral part of the cytoskeletal structure in dendritic spines, this result suggests a breakdown or alteration in the postsynaptic marker, consistent with a loss of connectivity. GFAP levels were increased by 31% (± 5.8; $P < 0.01$), and Aβ levels detected by the 10G4 antibody were increased by 132% (± 36.9; $P < 0.01$). This large increase in Aβ expression per terminal in association cortex, taken together with the increase measured in the Aβ-positive fraction (Figure 3B), indicates that Aβ accumulation in synaptic terminals is prominent in regions relatively unaffected by AD lesions compared to hippocampus and entorhinal cortex. The synapse-associated increase in GFAP suggests that glial changes occur around terminals expressing increased Aβ in AD cortex.

Table 1 illustrates that synaptic amyloid levels are related to atrophy and plaques in AD cases, with relatively high synaptic amyloid levels also measured in the demented Parkinson's case. Table 1 also reveals that the second control case, in which moderate atrophy and plaques were noted on the neuropathology report despite a MMSE of 29, also showed relatively high synaptic amyloid with our measure.

Western blots from representative P-2 samples in the cohort are shown in Figure 5. Trends were observed for a decrease in PSD-95 and increase in GFAP, but densitometric scanning did not reveal any significant differences between normal cases ($n = 5$) and AD cases ($n = 7$). In addition, no difference on Westerns was observed in the expression of synaptophysin or the 7A6 antigen in AD cases (data not shown), even with the addition of additional cases not in the present cohort. Western analysis would be expected to be less sensitive than flow cytometry, given that it is a one-dimensional measure that necessarily includes all of the nonsynaptosomal particles in the P-2. The increase in Aβ immunoreactivity measured by flow cytometry is supported by enzyme-linked immu-

nosorbent assay for amyloid β, which showed an increase in total Aβ from 77.49 pg/μg protein ($\pm$41, $n = 4$) to 126.03 pg/μg protein in AD cases ($\pm$66, $n = 6$).

A positive correlation between Aβ fluorescence and synaptosome size (forward scatter) in AD but not normal cases was also observed, and this correlation was highly significant despite the relatively small sample size ($r = 0.898$, $P < 0.0001$), ie, terminal size was increased in samples with higher Aβ expression (data not shown). This result is consistent with electron microscope observations of swollen processes and abnormal morphology in Aβ-positive terminals,[2,6] an interpretation of synaptic pathology associated with Aβ that is supported by the observation in some cases of disappearance of large synaptosomes (Figure 1B).

Discussion

Synapse loss and dysfunction in AD is well documented,[2,38] but the pathway(s) that lead to trimming of the neuronal arbor before cell death have not been resolved. Our results demonstrate synapse-associated Aβ labeling in AD terminals. Moreover, we observed the loss of a postsynaptic marker with preservation of three of four markers on the presynaptic side in AD synapses, accompanied by local glial change.

Amyloid plaques and neurofibrillary pathology occur relatively late in association neocortex, leading to the proposal that synapse loss in frontal and temporal cortex is the primary biological correlate of early cognitive deficits.[2,39] However, the degree of synapse loss that has been reported in frontal cortex is variable; some authors have observed significant loss early in AD,[40] whereas others have observed a biphasic change in which synaptic markers are actually increased in mild to moderate disease.[10] One explanation proposed for an initial increase is that early neuronal sprouting occurs in response to tau aggregation and failed axonal transport. An alternative explanation would be that Aβ induces aberrant sprouting as it does in animal models.[11,12] We observed slight SNAP-25 decreases in a few cases, but the net trend for an increase in the expression of presynaptic markers suggests that a sprouting response predominated in our sample. Interestingly, in animal models, presynaptic marker loss is not evident or limited.[11,12]

Studies in transgenic mice have shown that cognitive dysfunction and soluble Aβ levels rise months before the appearance of amyloid plaques,[41] and a body of evidence now suggests that soluble oligomeric forms of Aβ are more toxic than fibrils.[42–44] Intracellular accumulation of Aβ before extracellular deposition has been suggested as a mechanism for synaptic dysfunction and loss, and our results showing increased terminal Aβ are supported by electron microscope observations of Aβ42 accumulation in both pre- and postsynaptic compartments.[6] Recent observations that knife lesions of the perforant pathway in transgenic mice reduce extracellular amyloid deposits suggest that axonally transported APP is a likely source of intraterminal Aβ,[7] but the cellular localization of APP processing to Aβ remains unclear.

The N-terminal Aβ antibody used in the present studies does not distinguish between amyloid peptide species; however, we have been unable to demonstrate increased APP labeling with a series of APP monoclonal antibodies in addition to the 3E9 antibody results shown here. Importantly, localization of more soluble preamyloid has been difficult, presumably because of masked epitopes and/or peptide compartmentalization.[45] For example, GM1 ganglioside-bound amyloid, undetectable by common anti-Aβ antibodies without methanol extraction, has been isolated from diffuse plaques and suggested as a seed-forming species within lipid raft compartments.[46,47] In light of previous evidence, and in the absence of detection of other APP peptide species, the present results seem most likely to represent either increased APP C-terminal fragments that contain the Aβ sequence, or soluble Aβ peptide. Accumulations of Aβ oligomer, notably dimers, in lipid raft compartments in APP transgenic mice and AD brain[48] may, at least in part, reflect the increases observed in synaptic terminals in the present study.

The level of BACE in our assay was not affected by AD, which is in contrast to other studies in which increased BACE expression level and activity in AD cortex were observed.[49,50] Low levels of BACE signal in terminal regions compared to whole brain homogenates may be responsible for our inability to detect changes; however, our results are consistent with findings that show increased BACE activity but not BACE protein levels in mouse models of AD and in aged human cortex.[51]

Recent evidence indicates that astrocytes regulate the formation, maturation, and maintenance of synapses in the central nervous system,[36] and that the peripheral astrocyte process positioned next to the synaptic cleft represents a separate astroglial compartment.[37] In the present results, the increased expression of GFAP in the synaptosomal population is consistent with a maintenance role in which GFAP up-regulation occurs in response to initial localized damage and dysfunction in the synapse. A dynamic synapse maintenance role is supported by recent evidence that glial-derived cholesterol is responsible for enhancing the number of synapses in cultured neurons.[52,53] In addition, glial processes in the aging human brain have been observed to be wrapped tightly around synapses, leading to the suggestion that these processes aid in the phagocytosis and removal of terminals.[54]

A large body of evidence has shown that caspase activation and apoptosis are induced by Aβ proteins, but the precise contribution of caspase activation to Alzheimer pathology is unclear.[55] 7A6 antibody detects a mitochondrial antigen that is expressed in cells that have just begun to undergo apoptosis;[20] this antigen is not expressed in young adult rodents (data not shown). Because the mitochondria in the present study are in synaptic regions, the relatively high levels of labeling that we observe in the aged cohort in the present study (mean age, 83 years) may indicate that apoptotic changes occur in synaptic regions as a part of neuronal aging. Alternatively, some of the proapoptotic signal that we observe may represent a postmortem autolysis effect.

Because controls have slightly longer postmortem intervals in our cohort than do AD cases and no postmortem interval effect was observed (data not shown), 7A6 labeling presumably reflects premortem pathology.

The present observation that PSD-95 is decreased in AD synaptosomes on a per-terminal basis is backed by recent observations in our laboratory showing that PSD-95 decreases are greater than synaptophysin decreases in APPsw (Tg2576) transgenic mice[56] and in AD temporal cortex (Calon F, unpublished observations). These results are in line with previous work showing dramatic AD-related decreases in drebrin, a protein involved in synapse plasticity.[13–15] Like PSD-95, drebrin is a structural protein found in dendritic spines that is an important determinant of dendritic morphology,[57] leading to the proposal that caspase activation in neurites may induce disorganization of the actin filamentous network, including drebrin, with subsequent dyswiring between pre- and postsynapses.[15] Determining the sequence of synaptic changes from observations at a single postmortem time point is difficult; however, our ability to measure postsynaptic marker loss that is not accompanied by significant presynaptic loss in a synaptosome preparation may indicate that the postsynaptic element is more vulnerable than the presynaptic side and suggests it may degrade first. Also, early and larger alterations in postsynaptic versus presynaptic mRNA levels have been observed in aging dual APPsw and presenilin-1 transgenic mice.[58]

Considered together, the present findings in AD synapse regions suggests a pathway for synapse degeneration in which amyloid accumulation results in synaptic dysfunction that is manifested by selective pre- and postsynaptic changes in surviving terminals. The actin filamentous network in the more vulnerable postsynaptic side begins to be degraded, and the decline in synapse function induces a feedback response in which GFAP up-regulates in supporting astrocyte processes, and expression of exocytotic proteins may increase on the presynaptic side. This sequence provides a mechanism by which intracellular Aβ could result in *trans*-synaptic spread of AD pathology from presynaptic sites to postsynaptic sites.[5,8] Continued investigation into pre- and postsynaptic mediators of Aβ damage and identification of the amyloid species present in affected terminals is needed for more detailed answers about mechanisms of initial synaptic damage before cell death in AD. Future studies including mild cognitive impairment cases and a range of dementia severity will be important to clarify the sequence of changes observed in the present study. Flow cytometry analysis provides the necessary precise quantification and definitive synaptic localization in surviving terminals to answer important questions about the sequence of events before the disappearance of synapses.

References

1. Hardy J, Selkoe DJ: The amyloid hypothesis of Alzheimer's disease: progress and problems on the road to therapeutics. Science 2002, 297:353–356
2. Terry RD, Masliah E, Salmon DP, Butters N, DeTeresa R, Hill R, Hansen LA, Katzman R: Physical basis of cognitive alterations in Alzheimer's disease: synapse loss is the major correlate of cognitive impairment. Ann Neurol 1991, 30:572–580
3. Lue LF, Kuo YM, Roher AE, Brachova L, Shen Y, Sue L, Beach T, Kurth JH, Rydel RE, Rogers J: Soluble amyloid beta peptide concentration as a predictor of synaptic change in Alzheimer's disease. Am J Pathol 1999, 155:853–862
4. Mucke L, Masliah E, Yu GQ, Mallory M, Rockenstein EM, Tatsuno G, Hu K, Kholodenko D, Johnson-Wood K, McConlogue L: High-level neuronal expression of abeta 1-42 in wild-type human amyloid protein precursor transgenic mice: synaptotoxicity without plaque formation. J Neurosci 2000, 20:4050–4058
5. Gouras GK, Tsai J, Naslund J, Vincent B, Edgar M, Checler F, Greenfield JP, Haroutunian V, Buxbaum JD, Xu H, Greengard P, Relkin NR: Intraneuronal Abeta42 accumulation in human brain. Am J Pathol 2000, 156:15–20
6. Takahashi RH, Milner TA, Li F, Nam EE, Edgar MA, Yamaguchi H, Beal MF, Xu H, Greengard P, Gouras GK: Intraneuronal Alzheimer abeta42 accumulates in multivesicular bodies and is associated with synaptic pathology. Am J Pathol 2002, 161:1869–1879
7. Lazarov O, Lee M, Peterson DA, Sisodia SS: Evidence that synaptically released beta-amyloid accumulates as extracellular deposits in the hippocampus of transgenic mice. J Neurosci 2002, 22:9785–9793
8. Sheng JG, Price DL, Koliatsos VE: Disruption of corticocortical connections ameliorates amyloid burden in terminal fields in a transgenic model of Abeta amyloidosis. J Neurosci 2002, 22:9794–9799
9. Selkoe DJ: Alzheimer's disease is a synaptic failure. Science 2002, 298:789–791
10. Mukaetova-Ladinska EB, Garcia-Siera F, Hurt J, Gertz HJ, Xuereb JH, Hills R, Brayne C, Huppert FA, Paykel ES, McGee M, Jakes R, Honer WG, Harrington CR, Wischik CM: Staging of cytoskeletal and beta-amyloid changes in human isocortex reveals biphasic synaptic protein response during progression of Alzheimer's disease. Am J Pathol 2000, 157:623–636
11. King DL, Arendash GW: Maintained synaptophysin immunoreactivity in Tg2576 transgenic mice during aging: correlations with cognitive impairment. Brain Res 2002, 926:58–68
12. Hu L, Wong TP, Cote SL, Bell KF, Cuello AC: The impact of Abeta-plaques on cortical cholinergic and non-cholinergic presynaptic boutons in Alzheimer's disease-like transgenic mice. Neuroscience 2003, 121:421–432
13. Harigaya Y, Shoji M, Shirao T, Hirai S: Disappearance of actin-binding protein, drebrin, from hippocampal synapses in Alzheimer's disease. J Neurosci Res 1996, 43:87–92
14. Hatanpaa K, Isaacs KR, Shirao T, Brady DR, Rapoport SI: Loss of proteins regulating synaptic plasticity in normal aging of the human brain and in Alzheimer disease. J Neuropathol Exp Neurol 1999, 58:637–643
15. Shim KS, Lubec G: Drebrin, a dendritic spine protein, is manifold decreased in brains of patients with Alzheimer's disease and Down syndrome. Neurosci Lett 2002, 324:209–212
16. Yang F, Sun X, Beech W, Teter B, Wu S, Sigel J, Vinters HV, Frautschy SA, Cole GM: Antibody to caspase-cleaved actin detects apoptosis in differentiated neuroblastoma and plaque-associated neurons and microglia in Alzheimer's disease. Am J Pathol 1998, 152:379–389
17. Ivins KJ, Bui ET, Cotman CW: Beta-amyloid induces local neurite degeneration in cultured hippocampal neurons: evidence for neuritic apoptosis. Neurobiol Dis 1998, 5:365–378
18. Mattson MP, Duan W: "Apoptotic" biochemical cascades in synaptic compartments: roles in adaptive plasticity and neurodegenerative disorders. J Neurosci Res 1999, 58:152–166
19. Mak K, Yang F, Vinters HV, Frautschy SA, Cole GM: Polyclonals to beta-amyloid(1-42) identify most plaque and vascular deposits in Alzheimer cortex, but not striatum. Brain Res 1994, 667:138–142
20. Zhang C, Ao Z, Seth A, Schlossman SF: A mitochondrial membrane protein defined by a novel monoclonal antibody is preferentially detected in apoptotic cells. J Immunol 1996, 157:3980–3987
21. Dodd PR, Hardy JA, Oakley AE, Edwardson JA, Perry EK, Delaunoy

JP: A rapid method for preparing synaptosomes: comparison, with alternative procedures. Brain Res 1981, 226:107–118

22. Weiler MH, Gundersen CB, Jenden DJ: Choline uptake and acetylcholine synthesis in synaptosomes: investigations using two different labeled variants of choline. J Neurochem 1981, 36:1802–1812

23. Schmid I, Uittenbogaart CH, Giorgi JV: A gentle fixation and permeabilization method for combined cell surface and intracellular staining with improved precision in DNA quantification. Cytometry 1991, 12:279–285

24. Lim GP, Yang F, Chu T, Chen P, Beech W, Teter B, Tran T, Ubeda O, Ashe KH, Frautschy SA, Cole GM: Ibuprofen suppresses plaque pathology and inflammation in a mouse model for Alzheimer's disease. J Neurosci 2000, 20:5709–5714

25. Gylys KH, Fein JA, Cole GM: Quantitative characterization of crude synaptosomal fraction (P-2) components by flow cytometry. J Neurosci Res 2000, 61:186–192

26. Gylys KH, Fein JA, Tan AM, Cole GM: Apolipoprotein E enhances uptake of soluble but not aggregated amyloid-beta protein into synaptic terminals. J Neurochem 2003, 84:1442–1451

27. Gylys KH, Fein JA, Yang F, Cole GM: Enrichment of presynaptic and postsynaptic markers by size-based gating analysis of synaptosomes preparations from rat and human cortex. Cytometry 2004, 60A:90–96

28. Johnson MW, Chotiner JK, Watson JB: Isolation and characterization of synaptoneurosomes from single rat hippocampal slices. J Neurosci Methods 1997, 77:151–156

29. Wechsler A, Teichberg VI: Brain spectrin binding to the NMDA receptor is regulated by phosphorylation, calcium and calmodulin. EMBO J 1998, 17:3931–3939

30. Chicurel ME, Terrian DM, Potter H: mRNA at the synapse: analysis of a synaptosomal preparation enriched in hippocampal dendritic spines. J Neurosci 1993, 13:4054–4063

31. Nicholls DG: The glutamatergic nerve terminal. Eur J Biochem 1993, 212:613–631

32. Gylys KH, Fein JA, Cole GM: Caspase inhibition protects nerve terminals from in vitro degradation. Neurochem Res 2002, 27:465–472

33. Sudhof TC: The synaptic vesicle cycle: a cascade of protein-protein interactions. Nature 1995, 375:645–653

34. Kornau HC, Schenker LT, Kennedy MB, Seeburg PH: Domain interaction between NMDA receptor subunits and the postsynaptic density protein PSD-95. Science 1995, 269:1737–1740

35. Xue M, Zhang B: Do SNARE proteins confer specificity for vesicle fusion? Proc Natl Acad Sci USA 2002, 99:13359–13361

36. Slezak M, Pfrieger FW: New roles for astrocytes: regulation of CNS synaptogenesis. Trends Neurosci 2003, 26:531–535

37. Derouiche A, Anlauf E, Aumann G, Muhlstadt B, Lavialle M: Anatomical aspects of glia-synapse interaction: the perisynaptic glial sheath consists of a specialized astrocyte compartment. J Physiol Paris 2002, 96:177–182

38. Masliah E, Mallory M, Hansen L, DeTeresa R, Alford M, Terry R: Synaptic and neuritic alterations during the progression of Alzheimer's disease. Neurosci Lett 1994, 174:67–72

39. DeKosky ST, Scheff SW: Synapse loss in frontal cortex biopsies in Alzheimer's disease: correlation with cognitive severity. Ann Neurol 1990, 27:457–464

40. Masliah E, Mallory M, Alford M, DeTeresa R, Hansen LA, McKeel Jr DW, Morris JC: Altered expression of synaptic proteins occurs early during progression of Alzheimer's disease. Neurology 2001, 56:127–129

41. Kawarabayashi T, Younkin LH, Saido TC, Shoji M, Ashe KH, Younkin SG: Age-dependent changes in brain CSF, and plasma amyloid

(beta) protein in the Tg2576 transgenic mouse model of Alzheimer's disease. J Neurosci 2001, 21:372–381

42. Lambert MP, Barlow AK, Chromy BA, Edwards C, Freed R, Liosatos M, Morgan TE, Rozovsky I, Trommer B, Viola KL, Wals P, Zhang C, Finch CE, Krafft GA, Klein WL: Diffusible, nonfibrillar ligands derived from Abeta1-42 are potent central nervous system neurotoxins. Proc Natl Acad Sci USA 1998, 95:6448–6453

43. Walsh DM, Hartley DM, Kusumoto Y, Fezoui Y, Condron MM, Lomakin A, Benedek GB, Selkoe DJ, Teplow DB: Amyloid beta-protein fibrillogenesis. Structure and biological activity of protofibrillar intermediates. J Biol Chem 1999, 274:25945–25952

44. Klein WL, Krafft GA, Finch CE: Targeting small Abeta oligomers: the solution to an Alzheimer's disease conundrum? Trends Neurosci 2001, 24:219–224

45. Davies CA, Mann DM: Is the "preamyloid" of diffuse plaques in Alzheimer's disease really nonfibrillar? Am J Pathol 1993, 143:1594–1605

46. Kakio A, Nishimoto S, Yanagisawa K, Kozutsumi Y, Matsuzaki K: Interactions of amyloid beta-protein with various gangliosides in raft-like membranes: importance of GM1 ganglioside-bound form as an endogenous seed for Alzheimer amyloid. Biochemistry 2002, 41:7385–7390

47. Yanagisawa K, Odaka A, Suzuki N, Ihara Y: GM1 ganglioside-bound amyloid beta-protein (A beta): a possible form of preamyloid in Alzheimer's disease. Nat Med 1995, 1:1062–1066

48. Kawarabayashi T, Shoji M, Younkin LH, Wen-Lang L, Dickson DW, Murakami T, Matsubara E, Abe K, Ashe KH, Younkin SG: Dimeric amyloid beta protein rapidly accumulates in lipid rafts followed by apolipoprotein E and phosphorylated tau accumulation in the Tg2576 mouse model of Alzheimer's disease. J Neurosci 2004, 24:3801–3809

49. Li R, Lindholm K, Yang LB, Yue X, Citron M, Yan R, Beach T, Sue L, Sabbagh M, Cai H, Wong P, Price D, Shen Y: Amyloid beta peptide load is correlated with increased beta-secretase activity in sporadic Alzheimer's disease patients. Proc Natl Acad Sci USA 2004, 101:3632–3637

50. Holsinger RM, McLean CA, Beyreuther K, Masters CL, Evin G: Increased expression of the amyloid precursor beta-secretase in Alzheimer's disease. Ann Neurol 2002, 51:783–786

51. Fukumoto H, Rosene DL, Moss MB, Raju S, Hyman BT, Irizarry MC: Beta-secretase activity increases with aging in human, monkey, and mouse brain. Am J Pathol 2004, 164:719–725

52. Pfrieger FW, Barres BA: Synaptic efficacy enhanced by glial cells in vitro. Science 1997, 277:1684–1687

53. Ullian EM, Sapperstein SK, Christopherson KS, Barres BA: Control of synapse number by glia. Science 2001, 291:657–661

54. Adams I, Jones DG: Synaptic remodelling and astrocytic hypertrophy in rat cerebral cortex from early to late adulthood. Neurobiol Aging 1982, 3:179–186

55. Roth KA: Caspases, apoptosis, and Alzheimer disease: causation, correlation, and confusion. J Neuropathol Exp Neurol 2001, 60:829–838

56. Calon F, Lim GP, Yang F, Morihora T, Teter B, Ubeda O, Rostaing P, Triller A, Salem Jr N, Ashe KH, Frautschy SA, Cole GM: Docosahexaenoic acid protects from dendritic pathology in an Alzheimer's disease mouse model. Neuron 2004, 43:633–645

57. Shirao T, Sekino Y: Clustering and anchoring mechanisms of molecular constituents of postsynaptic scaffolds in dendritic spines. Neurosci Res 2001, 40:1–7

58. Dickey CA, Loring JF, Montgomery J, Gordon MN, Eastman PS, Morgan D: Selectively reduced expression of synaptic plasticity-related genes in amyloid precursor protein + presenilin-1 transgenic mice. J Neurosci 2003, 23:5219–5226